

Results on Identified Charged Hadrons from the PHENIX Experiment at RHIC

T. Chujo^a for the PHENIX Collaboration.

^aBrookhaven National Laboratory, Upton, NY 11973-5000, USA

Recent results on identified hadrons from the PHENIX experiment in Au+Au collisions at mid-rapidity at $\sqrt{s_{NN}} = 200$ GeV are presented. The centrality dependence of transverse momentum distributions and particle ratios for identified charged hadrons are studied.

1. Introduction and Experimental Setup

The physics motivation of the ultra-relativistic heavy-ion program at the Relativistic Heavy Ion Collider (RHIC) is to study nuclear matter at extremely high temperature and energy density with the hope to reach a new form of matter called the quark gluon plasma (QGP). Among the various probes of the QGP state, hadrons carry important information about the collision dynamics along with the spatial and temporal evolution of the system from the early stage of the collisions to the final state interactions.

For studies of hadron physics at RHIC, the PHENIX experiment [1] demonstrates good capability for particle identification (PID) for both charged hadrons (π^\pm , K^\pm , p , \bar{p} , d and \bar{d}) and neutral pions over a broad momentum range. The charged hadrons can be identified with time-of-flight measurements in two different detectors: (1) a high resolution Time-of-Flight wall (TOF) and, (2) an electro-magnetic calorimeter (EMC), in conjunction with the tracking system in the PHENIX central arm spectrometers and the beam counter, which provides the start timing and the event vertex determination. The tracking system in the central arm consists of drift chambers (DC), three layers of pad chambers (PC), and time expansion chambers (TEC). The PHENIX central arms cover $|\eta| < 0.35$ in pseudo-rapidity, and cover $\pi/4$ with the TOF and $3\pi/4$ by EMC in azimuth. The π/K and K/p separation can be achieved up to 2 and 4 GeV/c in p_T , respectively, using the TOF detector, which has a 120 ps timing resolution. Neutral pions are identified with the EMC via the $\pi^0 \rightarrow \gamma\gamma$ decay channel up to 10 GeV/c in p_T using the full statistics taken during Run II at RHIC in Au+Au collisions [2].

2. Experimental Results

We have measured the transverse momentum distributions for π^\pm , K^\pm , p and \bar{p} at mid-rapidity in Au+Au collisions at $\sqrt{s_{NN}} = 200$ GeV over a broad momentum range over various centrality selections. To identify the charged particles, the high resolution TOF counter is used in this analysis. We use about 4 million minimum bias events. The data

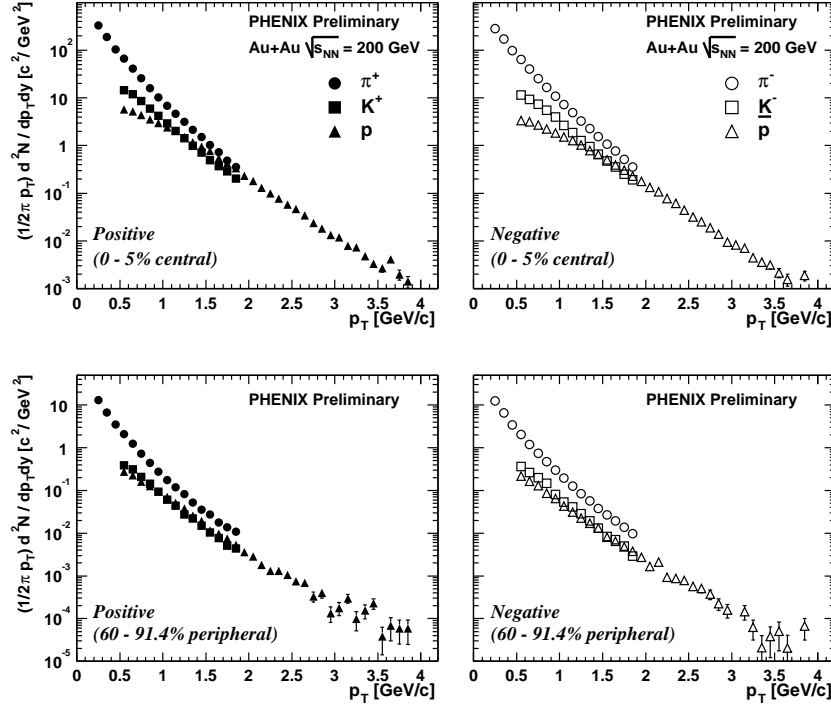


Figure 1. Transverse momentum distributions for pions (circles), kaons (squares) and p , \bar{p} (triangles) in the 0–5% most central events (upper panels) and 60–91.4% most peripheral events (lower panels) at $\sqrt{s_{NN}} = 200$ GeV in Au+Au collisions. The left panels show positive particles and the right panels show negative particles. The error bars are statistical only.

are classified into 11 centrality bins expressed in percent of the total inelastic cross section. The spectra for each particle species are corrected for geometrical acceptance, decay in flight, multiple scattering, and tracking efficiency using a single particle Monte Carlo simulation. A multiplicity-dependent track reconstruction efficiency is also determined and applied by embedding simulated tracks into real events.

The upper two panels in Figure 1 show the p_T distributions for identified hadrons in the most central events (0–5%) in 200 GeV Au+Au collisions for positive (left) and negative (right) particles. The lower two panels show the most peripheral events (60–91.4%). In each panel, the data are presented up to 1.8 GeV/ c for charged pions and kaons, and 3.8 GeV/ c for p and \bar{p} . In the low p_T region of the most central events, the data indicate that the inverse slope increases with the particle mass. Also, the shape of the p and \bar{p} spectra have a shoulder-arm shape while the pion spectra have a concave shape. On the other hand, in the most peripheral events, the spectra are almost parallel to each other. This mass dependence of the slopes and shapes of the spectra for protons in the central events can be explained by a radial flow picture. At around 2.0 GeV/ c in central events,

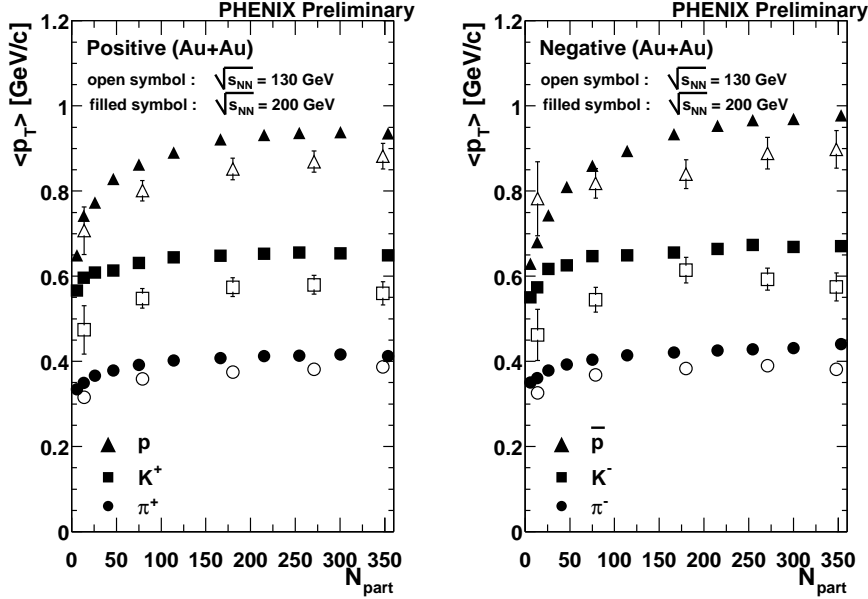


Figure 2. Mean transverse momentum for identified charged hadrons as a function of N_{part} for protons and anti-protons (triangles), kaons (squares) and pions (circles). The left panel shows positive particles and right panel shows negative particles. The open symbols indicate the data for 130 GeV [3] while the filled symbols indicate the data for 200 GeV in Au+Au collisions.

the proton yield becomes comparable to the pion yield. A similar behavior is also seen for negatively charged particles.

In order to quantify the observed mass dependence of the slopes, the mean transverse momenta $\langle p_T \rangle$ are extracted for 11 centrality selections and for each particle species. The p_T spectra are extrapolated to below and above the measured range using a power law function for pions, an m_T exponential function for kaons, and a Boltzmann function for p and \bar{p} . In Figure 2, the centrality dependence of $\langle p_T \rangle$ for identified charged hadrons are shown together with the 130 GeV data points [3]. In both the 200 GeV and 130 GeV data, $\langle p_T \rangle$ for all particle species increases from the most peripheral to the most central events and also increases with particle mass. The dependence of $\langle p_T \rangle$ on particle mass suggests the existence of a collective hydrodynamical expansion. The dependence on the number of participant nucleons (N_{part}) calculated using a Glauber model [4] may be due to an increasing radial expansion from peripheral to central events.

Particle composition at high p_T is also interesting in order to understand baryon production and transport, system evolution, and the interplay between soft processes and jet quenching in hard processes. In Figure 3, the p/π and \bar{p}/π ratios are shown. For the denominator of the ratio p/π and \bar{p}/π , we use two independent measurements with different subsystems: (1) p_T spectra for π^\pm up to 2 GeV/c identified using the TOF, (2)

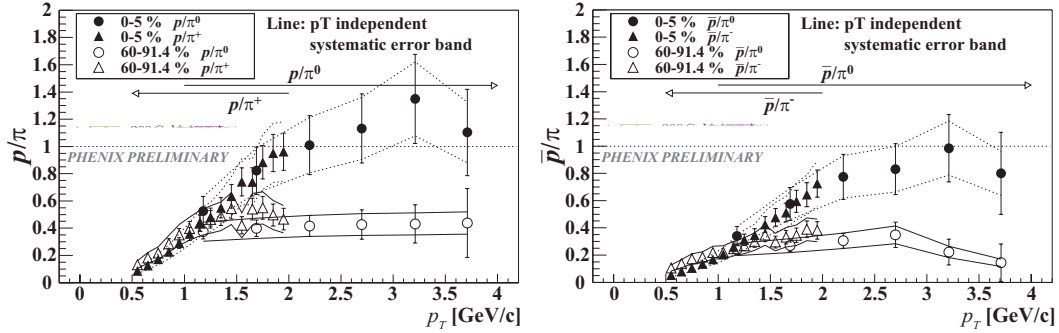


Figure 3. p/π (left) and \bar{p}/π (right) ratios as a function of p_T for the 0–5 % and 60–91.4% centrality selections. Lines along the data points show the p_T -independent systematic error bands. The error bars show the statistical and p_T -dependent systematic errors, summed in quadrature.

neutral pions results from 1 GeV/ c to 3.8 GeV/ c measured using the EMC. Both the p/π and \bar{p}/π ratios have a clear centrality dependence. The data shows that these ratios in central collisions reach unity at a p_T of 2~3 GeV/ c , while they saturate at around p_T of 0.3 – 0.4 in peripheral collisions. This observed behavior in central events may be attributed to the composition of two effects including a larger flow effect for protons (and \bar{p}) compared to pions, and a pion suppression effect at high p_T [5].

3. Summary

We present results on identified hadrons in Au+Au collisions at $\sqrt{s_{NN}} = 200$ GeV at mid-rapidity over different centrality selections from the PHENIX experiment. The transverse momentum distributions for π^\pm , K^\pm , p , \bar{p} , d , and \bar{d} are measured and we observe a mass dependence of the slopes and shapes of the identified charged spectra in central events. However, they are almost parallel to each other in the most peripheral events. Also, the mean transverse momentum for all particle species increases from peripheral to central events, and with particle mass. The ratios p/π and \bar{p}/π up to 3.8 GeV/ c are also measured by using the combined results for charged and neutral pions. In central collisions, the ratio reaches unity at a p_T of 2~3 GeV/ c and saturates at a p_T around 0.3 – 0.4 GeV/ c in peripheral collisions.

REFERENCES

1. PHENIX Collaboration, Nucl. Inst. to be submitted.
2. D. G. D’Enterria, for the PHENIX Collaboration, hep-ex/0209051.
3. K. Adcox et al., Phys. Rev. Lett. **88**, 242301 (2002).
4. K. Adcox et al., Phys. Rev. Lett. **86**, 3500 (2002).
5. K. Adcox et al., Phys. Rev. Lett. **88**:022301, (2002).